

# Dynamic charge oscillation in a quantum conductor driven by ultrashort voltage pulses

Lucas Mazzella and Seddik Ouacel\*

*Université Grenoble Alpes, CNRS, Grenoble INP, Institut Néel, Grenoble 38000, France*

Inès Safi\*

*Laboratoire de Physique des Solides, CNRS UMR 5802-Université Paris-Sud, Université Paris-Saclay, France*

(Dated: March 16, 2026)

Time-dependent driving with ultrashort voltage pulses brings quantum conductors into the non-adiabatic transport regime, where novel dynamical effects emerge. An example of this physics occurs in interferometric systems, where the transmitted charge oscillates as a function of the charge injected by an ultrashort voltage pulse. This behavior has been predicted in a variety of setups, including Fabry-Pérot and Mach-Zehnder interferometers, and more recently in quantum dots. It is commonly interpreted as resulting from interference between different propagating paths taken by the injected excitation. In this letter, we fully generalize the derivation of such dynamic charge oscillations beyond interferometric devices for a generic quantum conductor with the single assumption that its DC current is sublinear at large bias. Strikingly, they also extend perturbatively to strongly correlated conductors, showing in particular their robustness against arbitrarily strong Coulomb interactions. To illustrate the generality of our approach, we analyze in detail the case of a quantum point contact in the fractional quantum Hall regime, which fulfills the sublinearity condition. We demonstrate that this non-interferometric system exhibit dynamic charge oscillation. Finally, we propose a complementary interpretation of this phenomenon, rooted in the photo-assisted probabilities associated with the voltage pulse.

## I. INTRODUCTION

Recent advances in electron quantum optics have enabled the on-demand generation and coherent control of single-electron excitations, allowing the transposition of quantum optics paradigms to condensed matter systems through the manipulation of electrons in ballistic conductors [1–6].

Key achievements in this field include the controlled injection of electrons using voltage pulses that generate plasmonic excitations [1, 2], as well as the use of Lorentzian voltage pulses producing single-electron minimal excitations (Levitons) [7, 8]. These states were subsequently characterized experimentally through shot-noise measurements [9]. In addition, quantum state tomography has provided a full reconstruction of their coherence properties [10, 11], while time-resolved techniques have enabled the direct observation of propagating single-electron wave packets and the determination of their speed [12–14].

These advances have established precise control over single-electron excitations in ballistic conductors and paved the way for investigations into quantum interference effects and novel dynamical aspects [15]. Interference phenomena constitute the cornerstone of quantum physics, embodying the fundamental wave-particle complementarity that governs electronic transport in mesoscopic systems. For decades, such experiments were predominantly limited to the DC regime, where electrons are

injected as a continuous, temporally uncontrolled stream from voltage-biased contacts. The precise temporal control over single-electron pulses, enabling manipulation of both their shape and properties, has opened new frontiers [13]. Recent experiments have demonstrated interference with Leviton pulses and their coherent manipulation in graphene Mach-Zehnder interferometer (MZI) [16]. Related works [17, 18] further showed that similar interference effects can be exploited in Fabry-Pérot interferometers for quantum sensing applications. In addition, it has been shown that injecting pulses as short as 30 ps in a 14  $\mu m$  long MZI enables access to a non-adiabatic regime where internal timescales of the device are probed [19]. These developments have brought the dynamical aspects of quantum transport within experimental reach. One striking phenomenon of such dynamical effects is the oscillation of the transmitted charge as a function of the injected charge of the pulse when ultrashort voltage pulses are injected into interferometric systems [15, 20–23]. In what follows, we will refer to this effect as dynamic charge oscillations. Originally predicted for Fabry-Pérot and Mach-Zehnder interferometers [15], dynamic charge oscillations were later extended to tunnel-coupled wires [21]. More recently, a theoretical work showed that similar effects are also expected in quantum dots [22], thus questioning the conventional interfering-path picture. Importantly, all those works do not take into account Coulomb interactions, which may act as a source of decoherence and thus reduce interference visibility [24, 25].

In this work, we propose a general derivation of this dynamic charge oscillation. We consider either noninteracting systems with arbitrary transmission [20, 26]

---

\* mohamed-seddik.ouacel@neel.cnrs.fr

or arbitrary strongly correlated systems or quantum circuits in the weak-transmission regime, whose description falls within the Unifying Non-Equilibrium Perturbative (UNEP) approach [27–30]. Starting from the common expression obtained for the photo-assisted current, we show that dynamic charge oscillations are expected in any quantum conductor with a sublinear DC characteristic. This demonstrates that they are not limited to interferometers but also occurs in other types of devices. Moreover, they appear to be robust against Coulomb interaction. This is attributed to the extension of the side-band transmission picture in terms of correlated states showing coherent quantum superposition. Thus, we propose a complementary interpretation of dynamic charge oscillations that originate from oscillations of the photo-assisted probabilities associated with the AC excitation, rather than the traditional interferometry picture. To further support our argument, we study a non-interferometric system subject to a Lorentzian pulse with a finite width, a quantum point contact in the fractional quantum Hall (FQH) regime. It leads to clear dynamic charge oscillations in the short pulse limit, supporting our claim that the sublinearity of the DC characteristic is sufficient to observe dynamic charge oscillations.

## II. QUANTUM CONDUCTOR IN THE SHORT PULSE LIMIT

We start from a minimal description of a generic quantum conductor, characterized by its DC current–voltage relation  $I_{\text{dc}}(\omega)$  where  $\omega = \frac{eV}{\hbar}$  is a frequency associated with the DC voltage  $V$ . When driven by a time-dependent voltage pulse  $V(t)$ , the Fermi sea acquires an additional phase  $\varphi(t) = \frac{e}{\hbar} \int_{-\infty}^t dt' V(t')$  that corresponds to the injection of a total charge

$$q = \int_{-\infty}^{+\infty} dt \frac{eV(t)}{h} = \frac{\varphi(t = +\infty)}{2\pi}. \quad (1)$$

For simplicity, we have written the Josephson type relations obeyed by  $\omega$  and  $\varphi(t)$  for a single channel of independent electrons with charge  $e$ , noting that the formalism readily generalizes to fractional charges, Cooper pairs or multichannel systems [27, 28, 30].

In the following, we focus on the ultrashort-pulse limit, where the pulse duration is shorter than any internal timescale of the conductor. In that regime, the drive can be approximated as  $V(t) = V \delta(t)$ , leading to a phase  $\varphi(t) = 2\pi q \theta(t)$ , where  $\theta(t)$  denotes the Heaviside step function. The excitation generated by the pulse is encoded in the Fourier transform of the phase factor, which defines the photoassisted amplitudes

$$p(\omega) = \int_{-\infty}^{+\infty} e^{-i\varphi(t)} e^{i\omega t} dt, \quad (2)$$

whose squared modulus  $|p(\omega)|^2$  (or, for periodic drives, the discrete weights  $|p_l|^2$  with integer  $l$ ) gives the probability to absorb or emit a photon at frequency  $\omega$  [31, 32].

We study the transmitted charge  $\bar{n}$ , which can be expressed through the photoassisted relation

$$e\bar{n} = \int_{-\infty}^{+\infty} \frac{d\omega}{2\pi} |p(\omega)|^2 I_{\text{dc}}(\omega). \quad (3)$$

For non-interacting conductors, Eq. (3) is exact [20, 26] and has been used in all previous derivations of dynamic charge oscillations [21, 22, 33]. Remarkably, it has been shown to hold in full generality within the UNEP framework for strongly correlated quantum conductors or circuits, including superconducting correlations and Josephson junctions [27]. While restricted to a weak enough current, it has been extended to non-thermal states [30] and to Josephson type relations that might be modified by correlations. Eq. (3) will serve as our starting point. It expresses the transmitted charge induced by a time-dependent drive through a continuous superposition of the DC characteristic  $I_{\text{dc}}(\omega)$  weighted by the probabilities  $|p(\omega)|^2$  to exchange photons at frequency  $\omega$ . This extends fully the side-band transmission for single electron states under a periodic voltage [26] to non-periodic drives with which many-body correlated states exchange an energy  $\hbar\omega$  [28–30].

To evaluate Eq. (3) in the short-pulse limit, we introduce a standard regularization.

$$p_\epsilon(\omega) = \int_{-\infty}^{+\infty} e^{-i\varphi(t)} e^{i\omega t} e^{-\epsilon|t|} dt$$

$$e\bar{n}_\epsilon = \int_{-\infty}^{+\infty} \frac{d\omega}{2\pi} |p_\epsilon(\omega)|^2 I_{\text{dc}}(\omega) \quad (4)$$

such that  $\lim_{\epsilon \rightarrow 0} \bar{n}_\epsilon = \bar{n}$ . With  $\varphi(t) = 2\pi q \theta(t)$  one finds

$$|p_\epsilon(\omega)|^2 = \frac{2}{\omega^2 + \epsilon^2} - \frac{e^{2i\pi q}}{(\omega - i\epsilon)^2} - \frac{e^{-2i\pi q}}{(\omega + i\epsilon)^2}. \quad (5)$$

Substituting into Eq. (3) gives three terms. For the last two, an integration by parts yields

$$\int_{-\infty}^{+\infty} d\omega \frac{I_{\text{dc}}(\omega)}{(\omega \pm i\epsilon)^2} = \int_{-\infty}^{+\infty} d\omega \frac{G_{\text{dc}}(\omega)}{\omega \pm i\epsilon},$$

where  $G_{\text{dc}}(\omega) = \frac{dI_{\text{dc}}}{d\omega}(\omega)$  is the rescaled conductance that matches the transmission probabilities up to a factor  $2\pi$  in the non-interacting case. The boundary term  $[I_{\text{dc}}(\omega)/\omega]_{-\infty}^{+\infty}$  vanishes provided the DC characteristic is sublinear at large DC bias, i.e.

$$\lim_{\omega \rightarrow \pm\infty} \frac{I_{\text{dc}}(\omega)}{\omega} = 0. \quad (6)$$

Taking the limit  $\epsilon \rightarrow 0$  and using the Sokhotski–Plemelj formula then gives:

$$e\bar{n} = \frac{1}{\pi} \text{P.V.} \int_{-\infty}^{+\infty} d\omega \frac{G_{\text{dc}}(\omega)}{\omega} [1 - \cos(2\pi q)] + G_{\text{dc}}(0) \sin(2\pi q). \quad (7)$$

Eq. (7) relies on only two assumptions: (i) the photo-assisted form of Eq. (3), whose domain of validity has already been discussed and (ii) the sublinearity of the DC characteristic. The linear contribution to  $I_{\text{dc}}(\omega)$ , if present, can be treated separately, while Eq. (7) applies to the remaining nonlinear part of  $I_{\text{dc}}(\omega)$ .

Our derivation is independent on the microscopic details of the system. This unifies the predictions of dynamic charge oscillation reported in previous works in four distinct non-interacting systems [21, 22, 33]: Fabry-Pérot interferometers, MZIs, tunnel-coupled wires, and quantum dots. A detailed verification is provided in Supplementary material, demonstrating that our expression in Eq. (7) reproduces all these results in the ultrashort pulse limit. In those work, dynamic charge oscillation are interpreted as an interference phenomenon between different propagating paths. Strikingly, our derivation extends to non-interferometric devices showing that this is a universal phenomenon in quantum conductors driven with ultrashort voltage pulse.

Nonetheless, this universality covers strong electronic or superconducting correlations within the UNEP framework demonstrating the robustness of dynamic charge oscillations against Coulomb interaction in contrast with interferometric picture. This is in agreement with recent results for the Mach-Zehnder interferometer restricted to weak interaction [34].

In Sec. III, we illustrate this generalization by analyzing a quantum point contact (QPC) in the fractional quantum Hall (FQH) regime driven by a Lorentzian pulse of finite width.

### III. QUANTUM POINT CONTACT IN THE FRACTIONAL QUANTUM HALL REGIME

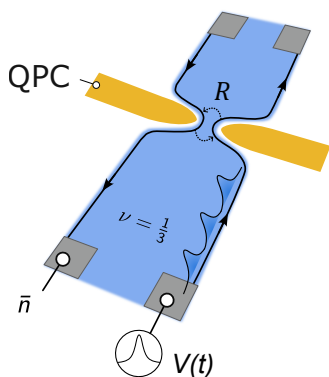


FIG. 1. Schematic of a QPC in the FQH edges. Electrons are injected by a periodic train of voltage pulses  $V(t)$  applied to an Ohmic contact, inducing the backscattered charge  $\bar{n}$ .

In this section we consider Laughlin FQH edges at simple filling factor  $\nu$  described by a Tomonaga-Luttinger Liquid with a weakly backscattering QPC (see Fig. 1a).

The DC backscattering current can be written as [35]

$$I_{\text{dc}}(\omega) = R e^* \frac{\omega_{\text{th}}}{\pi \Gamma(2\delta)} \left( \frac{\omega_c}{4\pi^2 \omega_{\text{th}}} \right)^{2(1-\delta)} \times \left| \Gamma \left( \delta + i \frac{\omega}{2\pi \omega_{\text{th}}} \right) \right|^2 \sinh \left( \frac{\omega}{2\omega_{\text{th}}} \right) \quad (8)$$

where  $\omega = e^*V/\hbar$  with  $e^*$  the quasiparticle charge,  $\delta$  the scaling dimension,  $\omega_{\text{th}} = k_B T/\hbar$  the thermal frequency,  $R$  the QPC reflection coefficient, and  $\omega_c$  a high-energy cutoff. To be specific, we choose  $\nu = \delta = e^*/e = 1/3$ ,  $R = 0.01$ . We also fix a thermal frequency  $\omega_{\text{th}} = 0.01 \omega_c$  to remain within the validity domain of the weak-backscattering description [36] (see End Matter 2 a). The resulting DC backscattering current is shown in Fig. 2. The thermal frequency  $\omega_{\text{th}}$  separates two distinct regimes. For  $\omega \ll \omega_{\text{th}}$ , the energy injected by the DC drive is smaller than the thermal energy. Quasiparticle excitations with energies of order  $k_B T$  are already thermally populated at the QPC, so that backscattering processes are effectively thermally activated. The applied voltage merely biases these pre-existing fluctuations, leading to a linear voltage bias characteristic, as shown by the green dashed line. In contrast, for  $\omega \gg \omega_{\text{th}}$ , quasiparticles are emitted at energies fixed by the DC drive. Thermal fluctuations are irrelevant at this energy scale. Therefore, the QPC probes the intrinsic quantum correlations of the fractional edge. The resulting backscattering current exhibits a non-linear power-law dependence on the bias, characteristic of chiral Luttinger-liquid behavior (see the blue dashed line). It clearly satisfies the sublinearity condition in Eq.(6), which, as noted above, is the key condition for observing dynamic charge oscillations in the ultrashort pulse limit.

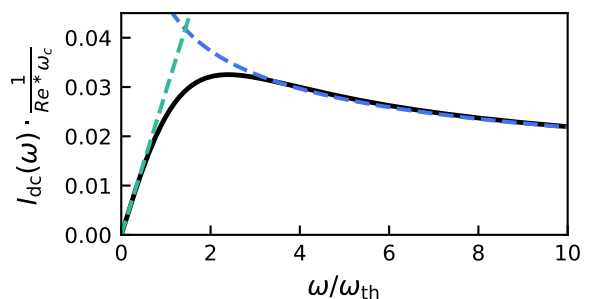


FIG. 2. DC backscattering current at the QPC with  $R = 0.01$ ,  $\nu = \delta = 1/3$  and  $\omega_{\text{th}} = 0.01 \cdot \omega_c$ . The green dotted line represents the equilibrium regime  $\omega \ll \omega_{\text{th}}$ . The blue dotted line represents the non-equilibrium regime  $\omega \gg \omega_{\text{th}}$ .

*a. Driven regime.* Having established the DC response and its sublinearity, we now consider a periodic train of Lorentzian voltage pulses of width  $\tau$  and period

$T_0$ ,

$$eV(t) = \sum_{n=-\infty}^{+\infty} \frac{2q\hbar\tau}{\tau^2 + (t - nT_0)^2}, \quad (9)$$

which injects a charge  $qe$  per pulse. The single-pulse limit is recovered for  $T_0 \rightarrow \infty$  at fixed  $\tau$ . In the UNEP framework [30], the backscattered charge per period reads

$$e\bar{n} = \frac{2\pi}{\Omega_0} \sum_{l=-\infty}^{+\infty} |p_l|^2 I_{dc}[(l+q)\Omega_0], \quad \Omega_0 = \frac{2\pi}{T_0}, \quad (10)$$

where

$$p_l = \frac{\Omega_0}{2\pi} \int_{-T_0/2}^{T_0/2} e^{-i\varphi(t)} e^{i\Omega_0 t} dt.$$

The shift  $l+q$  reflects the convention of removing the DC component of  $V(t)$  when defining the phase  $\varphi(t)$ . Eq. (10) is valid provided that we stay in the perturbative regime and in the validity domain of Eq. (8) as discussed in End Matter 2 a and 2 b.

*b. Numerical results* Eq. (10) is evaluated numerically, and the results are displayed in Fig. 3 for different values of pulse width  $\tau\omega_{th}$ . We choose the repetition frequency as  $\Omega_0 = 0.1\omega_{th}$ , such that  $\Omega_0 \ll \omega_{th}$  and  $\Omega_0 \ll 1/\tau$ . These conditions ensure that pulses are well separated in time and that the system fully relaxes between successive pulses. In this limit, the periodic drive effectively reduces to the single-pulse regime, allowing direct comparison of the numerical results with Eq. (7). For  $\tau\omega_{th} \gg 1$ , the backscattered charge  $\bar{n}$  follows the adiabatic limit (gray solid line in Fig. 3), where the voltage varies slowly compared to all intrinsic timescales of the conductor (see End Matter 2 c). When  $\tau\omega_{th} \sim 1$ , dynamic charge oscillations of  $\bar{n}$  as a function of the injected charge  $q$  appear and become more pronounced as the pulse width  $\tau$  is reduced. In the ultrashort-pulse limit  $\tau\omega_{th} \ll 1$ , the results are captured by the analytical expression of Eq. (7) (black solid line in Fig. 3). Notice that the analysis of the photoassisted current in [37] exhibits early signatures of oscillatory behavior at intermediate  $\tau\omega_{th}$  (e.g.,  $\tau\omega_{th} \sim 0.1$ ), although without explicitly linking this effect to dynamic charge oscillations. In the QPC, the crossover displayed in Fig. 3 as a function of  $\omega_{th}$  reproduces the behavior reported in interferometric devices: there,  $1/\omega_{th}$  effectively replaces the time of flight imbalance between paths [21, 33], or the finite lifetime of a quantum-dot level [22]. This behavior can be interpreted in the time domain by introducing the thermal coherence time  $\tau_{th} = 1/\omega_{th}$ , beyond which quasiparticle correlations are suppressed by thermal fluctuations. For long pulses,  $\tau \gg \tau_{th}$ , thermal fluctuations destroy coherence while the pulse propagates through the QPC, thereby smearing out the oscillations. In contrast, for short pulses,  $\tau \ll \tau_{th}$ , coherence is maintained throughout the passage of the pulse, allowing dynamic charge oscillations to emerge. Thereby, we

demonstrated that dynamic charge oscillations emerge in a non-interferometric device, matching the ultrashort-pulse prediction of Eq. (7).

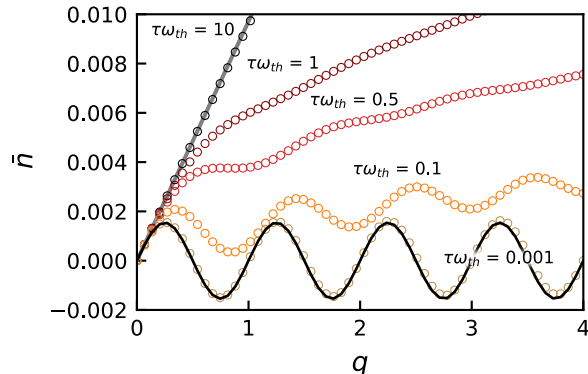


FIG. 3. Backscattered charge  $\bar{n}$  as a function of the injected charge  $q$  for Lorentzian pulses of various widths  $\tau$  at  $R = 0.01$ ,  $\nu = 1/3$ ,  $\delta = 1/3$ ,  $\omega_{th} = 0.01\omega_c$  and  $\Omega_0 = 10^{-3}\omega_c$ . Solid gray line: adiabatic limit. Solid black line: ultrashort pulse limit given by Eq. (7).

#### IV. INTERPRETATION OF DYNAMIC CHARGE OSCILLATIONS

The standard interpretation of dynamic charge oscillations relies on interference between different propagating paths [15, 23]. However, since we predict dynamic charge oscillations in non-interferometric systems as well, a more general interpretation applicable to both cases is required. A closer inspection of the calculation in Sec. I reveals that the oscillating term originates directly from the phase factor, as shown in Eq. (5). This feature is inherent to the excitation generated by the voltage pulse and does not depend on the specific quantum system under consideration. Our interpretation is therefore that the origin of dynamic charge oscillations lies in the oscillatory behavior of photo-assisted probabilities, which we are able to probe thanks to the sublinearity of the device. Interference is one possible mechanism leading to sublinear DC characteristic, but other energy-dependent processes can play the same role, such as tunneling in the case of a QPC in the FQH regime. This explains why dynamic charge oscillations manifest in different systems.

To illustrate our interpretation, we write the expression of the photoassisted probabilities  $|p_l|^2$  in the short-pulse limit for a periodic train of pulses [27, 30] (see End Matter 1 for the derivation):

$$|p_l|^2 = \frac{\sin^2(\pi q)}{\pi^2(l+q)^2} \quad (11)$$

First, the oscillations with the injected charge  $q$  appear in the expression of  $|p_l|^2$  as it was the case for the non-

periodic case in Eq. (5). In the non-interacting case,  $|p_l|^2$  represents the probability to exchange  $|l|$  photons with the pure AC source which shifts a single electron energy state from  $q\Omega_0$  to the Floquet state  $(l+q)\Omega_0$ . Within the UNEP framework, this simple picture can be extended to interacting systems by considering many-body correlated states instead of single electrons states [28–30]. We also consider a symmetric DC characteristic  $I(\omega) = -I(-\omega)$  such that Eq. (7) reduces to

$$\bar{n} = G_{\text{dc}}(0) \sin(2\pi q)$$

When  $q$  is an integer, Eq. (11) becomes  $|p_l|^2 = \delta_{l,-q}$ . One is left with a single term in the sum in Eq. (10) with  $|p_{-q}|^2 = 1$  leading to no transferred charge  $\bar{n}$  because the Floquet state has energy  $(l+q)\Omega_0 = 0$ .

When  $q = m + \frac{1}{2}$ , Eq. (11) gives  $|p_l|^2 = \frac{1}{\pi^2(l+m+\frac{1}{2})^2}$ .

In this case,  $|p_{l-m}|^2 = |p_{-l-m-1}|^2$  which means equal probabilities to populate the Floquet states with energies  $(l+1/2)\Omega_0$  and  $-(l+1/2)\Omega_0$ . The contributions of those two states to the transferred charge  $\bar{n}$  in Eq. (10) cancel each other because the DC current is odd such that  $\bar{n} = 0$ . The above considerations show that dynamic charge oscillations can be understood by considering the balance between the different Floquet states. It reinforces our claim that the origin of this phenomenon lies in the AC drive itself.

## V. CONCLUSION

We have demonstrated the universality of oscillations of the transmitted charge through quantum conductors (so called dynamic charge oscillations) as a function of the charge injected by ultrashort voltage pulses. Our analysis unifies, on one hand, non-interacting systems with arbitrary energy-dependent transmission amplitudes, and, on the other hand, strongly correlated systems or circuits described by the unified non-equilibrium perturbative theory. Remarkably, these oscillations extend beyond interferometers: they emerge as soon as the DC current-voltage characteristic is sublinear at large voltage, irrespective of the microscopic details of the system. Therefore, they persist even in the presence of strong interactions, in contrast to the oscillations observed in interferometers, where interactions typically induce decoherence. This robustness may originate from the generalization of the sideband transmission picture within the UNEP theory to correlated states, thereby indicating the presence of quantum coherence.

We have applied our approach to a quantum point contact in fractional quantum Hall edges in the

weak backscattering regime, described by a Tomonaga-Luttinger liquid for which the DC power-law characteristic satisfies the sublinearity condition. Considering a Lorentzian pulse with finite width, our numerical calculations capture the crossover from the adiabatic to the short-pulse regime and demonstrate the emergence of dynamic charge oscillations in the short-pulse limit. Notice that our approach extends to hierarchical FQH states as long as backscattering of a single quasiparticle species dominates. While the DC current keeps the same form [38] in the presence of edge interactions, we expect, however, that the latter induce fractionalization of the injected pulse, [1, 2, 5, 25, 30] whose spreading needs therefore to be reduced.

To date, these charge oscillations have not been observed experimentally. Our results provide a practical roadmap to identify platforms in which such dynamic charge oscillations could be detected on experimentally accessible timescales. Moreover, our framework can be extended to an initial non-equilibrium distribution due, for instance, to temperature gradients or three-terminal geometries and to hybrid systems with superconducting correlations (e.g., proximitized junctions), where Andreev processes and the BCS density of states naturally generate nonlinear DC responses.

Interestingly, our photoassisted approach could be extended to the time-resolved current, thereby revealing dynamical charge oscillations directly in the time domain. From this viewpoint, these oscillations can be rooted into interference effects analogous to time-domain braiding processes between anyons, as interpreted in "anyon-collider" [39, 40] or Hong-Ou-Mandel-type setups [41–43].

## ACKNOWLEDGMENTS

The authors acknowledge fruitful discussions with Pascal Degiovanni, Gwendal Fève and Aleksander Latyshev during the preparation of this manuscript. They thank Christopher Bauerle for carefully reading the manuscript and for valuable remarks. I.S. acknowledges the ANR grant "QuSig4QuSense" (ANR-21-CE47-0012). S.O. acknowledges funding from the European Innovation Council and SMEs Executive Agency under Grant Agreement 101185712, project ELEQUANT. L.M. acknowledges the program QuantEdu-France No. ANR-22-CMAS-0001 (France 2030).

Views and opinions expressed are those of the author(s) only and do not necessarily reflect those of the European Union or the granting authority. Neither the European Union nor the granting authority can be held responsible for them.

---

[1] Safi, Inès, Propriétés d'un fil quantique connecté à des

fil de mesure, Ann. Phys. Fr. **22**, 463 (1997).

- [2] I. Safi, A dynamic scattering approach for a gated interacting wire, *Eur. Phys. J. B* **12**, 451 (1999).
- [3] C. GRENIER, R. HERVÉ, G. FÈVE, and P. DEGIOVANNI, Electron quantum optics in quantum hall edge channels, *Modern Physics Letters B* **25**, 1053 (2011), <https://doi.org/10.1142/S0217984911026772>.
- [4] C. Bäuerle, D. C. Glattli, T. Meunier, F. Portier, P. Roche, P. Roulleau, S. Takada, and X. Waintal, Coherent control of single electrons: a review of current progress, *Rep. Prog. Phys.* **81**, 056503 (2018).
- [5] H. Kamata, N. Kumada, M. Hashisaka, K. Muraki, and T. Fujisawa, Fractionalized wave packets from an artificial tomonaga–luttinger liquid, *Nature Nanotechnology* **9**, 177 (2014).
- [6] H. Chakraborti, C. Gorini, A. Knothe, M.-H. Liu, P. Makk, F. D. Parmentier, D. Perconte, K. Richter, P. Roulleau, B. Sacépé, C. Schönenberger, and W. Yang, Electron wave and quantum optics in graphene, *Journal of Physics: Condensed Matter* **36**, 393001 (2024).
- [7] D. Ivanov, H. Lee, and L. Levitov, Coherent states of alternating current, *Phys. Rev. B* **56**, 6839 (1997).
- [8] J. Keeling, I. Klich, and L. S. Levitov, Minimal excitation states of electrons in one-dimensional wires, *Phys. Rev. Lett.* **97**, 116403 (2006).
- [9] J. Dubois, T. Jullien, F. Portier, P. Roche, A. Cavanna, Y. Jin, W. Wegscheider, P. Roulleau, and D. C. Glattli, Minimal-excitation states for electron quantum optics using levitons, *Nature* **502**, 659 (2013).
- [10] T. Jullien, P. Roulleau, B. Roche, A. Cavanna, Y. Jin, and D. C. Glattli, Quantum tomography of an electron, *Nature* **514**, 603 (2014).
- [11] R. Bisognin, A. Marguerite, B. Roussel, M. Kumar, C. Cabart, C. Chapdelaine, A. Mohammad-Djafari, J. M. Berroir, E. Bocquillon, B. Plaçais, A. Cavanna, U. Gennser, Y. Jin, P. Degiovanni, and G. Fève, Quantum tomography of electrical currents, *Nature Communications* **10**, 10.1038/s41467-019-11369-5 (2019).
- [12] G. Roussely, E. Arrighi, G. Georgiou, S. Takada, M. Schalk, M. Urdampilleta, A. Ludwig, A. D. Wieck, P. Armagnat, T. Kloss, X. Waintal, T. Meunier, and C. Bäuerle, Unveiling the bosonic nature of an ultrashort few-electron pulse, *Nature Communications* **9**, 10.1038/s41467-018-05203-7 (2018).
- [13] M. Aluffi, T. Vasselon, S. Ouacel, H. Edlbauer, C. Geffroy, P. Roulleau, D. C. Glattli, G. Georgiou, and C. Bäuerle, Ultrashort electron wave packets via frequency-comb synthesis, *Phys. Rev. Appl.* **20**, 034005 (2023).
- [14] S. Takada, G. Georgiou, J. Wang, Y. Okazaki, S. Nakamura, D. Pomaranski, A. Ludwig, A. D. Wieck, M. Yamamoto, C. Bäuerle, and N.-H. Kaneko, Eigenstate control of plasmon wavepackets with electron-channel blockade, *Nature Communications* **16**, 9942 (2025).
- [15] B. Gaury and X. Waintal, Dynamical control of interference using voltage pulses in the quantum regime, *Nat. Commun.* **5**, 3844 (2014).
- [16] A. Assouline, L. Pugliese, H. Chakraborti, S. Lee, L. Bernabeu, M. Jo, K. Watanabe, T. Taniguchi, D. C. Glattli, N. Kumada, H. S. Sim, F. D. Parmentier, and P. Roulleau, Emission and coherent control of levitons in graphene, *Science* **382**, 1260 (2023).
- [17] H. Bartolomei, E. Frigerio, M. Ruelle, G. Reborá, Y. Jin, U. Gennser, A. Cavanna, E. Baudin, J.-M. Berroir, I. Safi, P. Degiovanni, G. Ménard, and G. Fève, Time-resolved sensing of electromagnetic fields with single-electron interferometry, *Nature Nanotechnology* **20**, 596 (2025).
- [18] H. Souquet-Basiège, B. Roussel, G. Reborá, G. Ménard, I. Safi, G. Fève, and P. Degiovanni, Quantum sensing of time-dependent electromagnetic fields with single-electron excitations, *Phys. Rev. X* **15**, 031043 (2025).
- [19] S. Ouacel, L. Mazzella, T. Kloss, M. Aluffi, T. Vasselon, H. Edlbauer, J. Wang, C. Geffroy, J. Shaju, A. Ludwig, A. D. Wieck, M. Yamamoto, D. Pomaranski, S. Takada, N.-H. Kaneko, G. Georgiou, X. Waintal, M. Urdampilleta, H. Sellier, and C. Bäuerle, Electronic interferometry with ultrashort plasmonic pulses, *Nature Communications* **16**, 4632 (2025).
- [20] B. Gaury, J. Weston, M. Santin, M. Houzet, C. Groth, and X. Waintal, Numerical simulations of time-resolved quantum electronics, *Physics Reports* **534**, 1 (2014), numerical simulations of time-resolved quantum electronics.
- [21] J. Weston and X. Waintal, Towards realistic time-resolved simulations of quantum devices, *Journal of Computational Electronics* **15**, 1148 (2016).
- [22] T. Kloss and X. Waintal, Propagation of ultrashort voltage pulses through a small quantum dot, *Physical Review B* **111** (2025).
- [23] M. Saha, L. Horray, P. Portugal, and C. Flindt, Negative currents in fabry-pérot cavities are caused by interfering paths, *Phys. Rev. B* **112**, L081408 (2025).
- [24] P. Roulleau, F. Portier, D. C. Glattli, P. Roche, A. Cavanna, G. Faini, U. Gennser, and D. Mailly, Finite bias visibility of the electronic mach-zehnder interferometer, *Physical Review B - Condensed Matter and Materials Physics* **76**, 10.1103/PhysRevB.76.161309 (2007).
- [25] I. P. Levkivskiy and E. V. Sukhorukov, Dephasing in the electronic mach-zehnder interferometer at filling factor  $\nu = 2$ , *Phys. Rev. B* **78**, 045322 (2008).
- [26] G. Platero and R. Aguado, Photon-assisted transport in semiconductor nanostructures, *Physics Reports* **395**, 1 (2004).
- [27] I. Safi and E. V. Sukhorukov, Determination of tunneling charge via current measurements, *Eur. Phys. Lett.* **91**, 67008 (2010).
- [28] I. Safi, Time-dependent Transport in arbitrary extended driven tunnel junctions, *arXiv e-prints* (2014), [arXiv:1401.5950 \[cond-mat.mes-hall\]](https://arxiv.org/abs/1401.5950).
- [29] I. Safi, Driven strongly correlated quantum circuits and hall edge states: Unified photoassisted noise and revisited minimal excitations, *Phys. Rev. B* **106**, 205130 (2022).
- [30] I. Safi, Driven quantum circuits and conductors: A unifying perturbative approach, *Phys. Rev. B* **99**, 045101 (2019).
- [31] M. Moskalets and M. Büttiker, Floquet scattering theory of quantum pumps, *Phys. Rev. B* **66**, 205320 (2002).
- [32] J. Dubois, T. Jullien, C. Grenier, P. Degiovanni, P. Roulleau, and D. C. Glattli, Integer and fractional charge lorentzian voltage pulses analyzed in the framework of photon-assisted shot noise, *Phys. Rev. B* **88**, 085301 (2013).
- [33] B. Rossignol, T. Kloss, P. Armagnat, and X. Waintal, Toward flying qubit spectroscopy, *Phys. Rev. B* **98**, 205302 (2018).
- [34] P. Kumar, T. Kloss, and X. Waintal, Effect of electron-electron interactions on the propagation of ultrashort voltage pulses in a mach-zehnder interferometer (2026),

arXiv:2602.23973 [cond-mat.mes-hall].

- [35] X.-G. Wen, Edge transport properties of the fractional quantum hall states and weak-impurity scattering of a one-dimensional charge-density wave, *Phys. Rev. B* **44**, 5708 (1991).
- [36] I. Taktak and I. Safi, Ac driven fractional quantum hall systems: Uncovering unexpected features (2025), arXiv:2502.07622 [cond-mat.mes-hall].
- [37] J. Rech, D. Ferraro, T. Jonckheere, L. Vannucci, M. Sasseti, and T. Martin, Minimal excitations in the fractional quantum hall regime, *Phys. Rev. Lett.* **118**, 076801 (2017).
- [38] I. Safi, Time domain braiding of anyons revealed through a nonequilibrium fluctuation dissipation theorem (2025), arXiv:2510.10525.
- [39] C. Han, J. Park, Y. Gefen, and H.-S. Sim, Topological vacuum bubbles by anyon braiding, *Nature Communications* **7**, 11131 (2016).
- [40] J.-Y. M. Lee, C. Han, and H.-S. Sim, Fractional mutual statistics on integer quantum hall edges, *Phys. Rev. Lett.* **125**, 196802 (2020).
- [41] M. Ruelle, E. Frigerio, E. Baudin, J.-M. Berroir, B. Plaçais, B. Grémaud, T. Jonckheere, T. Martin, J. Rech, A. Cavanna, U. Gennser, Y. Jin, G. Ménard, and G. Fève, Time-domain braiding of anyons, *Science* **389**, eadm7695 (2025), <https://www.science.org/doi/pdf/10.1126/science.adm7695>.
- [42] S. Varada, C. Spånslätt, and M. Acciai, Exchange-phase erasure in anyonic hong-ou-mandel interferometry, *Phys. Rev. B* **111**, L201407 (2025).
- [43] A. Latyshev, I. Taktak, I. Mandal, and I. Safi, Hong-ou-mandel interferometry for fractional excitations: Unified framework and dip width scaling (2025), arxiv: 2509.07875.

## END MATTER

### 1. Expressions for $|p_l|^2$ in the short-pulse limit

In this section, we derive the expression of  $|p_l|^2$  for a periodic train of pulses in the short-pulse limit given in Eq. (11). We start with the expression of  $p_l^\eta$  for a periodic train of Lorentzian pulses [9].

$$p_l^\eta = \int_0^1 du \frac{\sin(\pi[u + i\eta])}{\sin(\pi[u - i\eta])} e^{2i\pi(l+q)u}$$

where  $\eta = \frac{\tau}{T}$  is the ratio between the width of the pulse and the period of repetition. Taking the limit  $\eta \rightarrow 0$  yields

$$\begin{aligned} p_l &= \int_0^1 du e^{2i\pi(l+q)u} \\ &= \frac{1}{2i\pi(l+q)} \left( e^{2i\pi(l+q)} - 1 \right) \\ &= \frac{\sin(\pi q)}{\pi(l+q)} e^{i\pi(l+q)}. \end{aligned}$$

Note that the case where  $q$  is an integer and  $l = q$  needs to be considered separately: it gives directly  $p_l = 1$ , which is fully consistent with the general formula. Taking the modulus square, we obtain Eq. (11)

$$|p_l|^2 = \frac{\sin(\pi q)^2}{\pi^2(l+q)^2}$$

### 2. Validity of the weak backscattering regime in the fractional quantum Hall (FQH) effect

#### a. DC regime

In order to stay in the weak backscattering regime (Eq. (8)), the DC drive must verify that the DC backscattering conductance is small with respect to the quantized conductance

$$\frac{e}{\hbar} |G_{\text{dc}}(\omega)| \ll \nu \frac{e^2}{\hbar}.$$

As discussed in Ref. [36], for  $\nu = \delta = e^*/e = 1/3$  and a reflection coefficient  $R = 0.01$ , this condition is safely ensured with a finite thermal cutoff satisfying  $\omega_{\text{th}} > 8 \times 10^{-3} \omega_c$ . For this reason, throughout this work, we fix the thermal frequency to the conservative value  $\omega_{\text{th}} = 0.01 \omega_c$ . Another limitation is that the TLL expression of the DC current applies only for an argument below the high-energy cutoff  $\omega_c$ . Consequently, when evaluating Eq. (10), we explicitly verify that the sum has converged for all contributions with  $\omega < 0.1 \omega_c$ .

*b. AC regime*

The UNEP framework extends Eq. (3) and (10) to interacting systems. The expressions for  $\omega$  and  $q$  in terms of external voltages might be more complicated for an initial non-equilibrium distribution, for instance due to temperature gradients or three-terminal geometries, but they are related universally to the effective phase felt by the scattering region. The conditions for the validity of the UNEP applied to a TLL model are discussed in Ref. [36]. Let us recall them here briefly using our notations.

We define the photo-current as

$$I_{\text{ph}} = \frac{e \bar{n}}{T_0},$$

and the corresponding photo-conductance as

$$G_{\text{ph}} = \frac{dI_{\text{ph}}}{dV_0}, \quad V_0 = q \frac{\hbar \Omega_0}{e^*}.$$

The perturbative treatment remains justified as long as

$$|G_{\text{ph}}| \ll \nu \frac{e^2}{h}.$$

Rewriting this condition in terms of charges yields

$$\left| \frac{d\bar{n}}{dq} \right| \ll 1$$

For all the injected charges  $q$  and pulse widths  $\tau$  we considered in this work,  $\left| \frac{d\bar{n}}{dq} \right| < 0.03$ , which satisfies this condition.

*c. Adiabatic limit*

We consider the limit of a long pulse ( $\Omega_0 \ll 1/\tau \ll \omega_{\text{th}}$ ), such that the current at time  $t$  is simply  $I_{\text{dc}}[V(t)]$  (for simplicity, we use here the voltage  $V$  as variable for the current instead of  $\omega$  as in the rest of this work).

$$e\bar{n} = \int_0^{T_0} dt I_{\text{dc}}[V(t)]$$

For small  $q$ , we can verify that  $e^*V(t)/\hbar \ll \omega_{\text{th}}$  (see Eq. (9)) such that  $I_{\text{dc}}[V(t)]$  becomes linear. We get

$$e\bar{n} = qe^*R \frac{|\Gamma(\delta)|^2}{\Gamma(2\delta)} \left( \frac{\omega_c}{4\pi^2\omega_{\text{th}}} \right)^{2(1-\delta)}$$